Water Management
Volume 165 Issue WM2

An assessment of DBM flood forecasting models
Vaughan and McIntyre

ice | proceedings

Proceedings of the Institution of Civil Engineers
Water Management 165 February 2012 Issue WM2
Pages 105–120 http://dx.doi.org/10.1680/wama.2012.165.2.105
Paper 1000103
Received 07/10/2010 Accepted 08/03/2011
Keywords: floods & floodworks/hydrology & water resource/mathematical modelling

ice Institution of Civil Engineers
publishing

An assessment of DBM flood forecasting models

Mike Vaughan MSc, MCIWEM, CWEM
Flood Forecasting Technical Specialist, Environment Agency, Worthing, UK; Postgraduate Research Student, Imperial College London, London, UK

Neil McIntyre MSc, PhD, MICE, CEng
Reader in Surface Water Hydrology, Department of Civil and Environmental Engineering, Imperial College London, London, UK

The data-based mechanistic (DBM) approach to modelling has been proposed as an alternative to the conceptual rainfall–runoff (CRR) models commonly used in operational flood forecasting systems. The approach offers a number of potential advantages, but questions remain over its applicability to lowland UK catchments, its use with 15 min data, the most appropriate model identification and real-time updating approaches, as well as how the flood forecasting performance of DBM models compares with that of CRR models. This paper applies the DBM approach to two catchments in south-east England, finding that it is as appropriate for lowland catchments and 15 min data as for the upland catchments and hourly data of previous studies. It also finds that continuous-time model identification is superior to discrete-time model identification, and that such models can be applied within a Kalman filter updating framework. Overall, however, the relatively simple application of DBM modelling could not improve upon the performance of a more complex CRR model, indicating that further work is required to exploit the potential of the DBM modelling framework to operational flood forecasting.

Notation

a_i	transfer function denominator coefficients
b_i	transfer function numerator coefficients
c	scaling coefficient in effective rainfall transformation
$\boldsymbol{F}$	state space model transition parameter matrix
$\boldsymbol{g}$	state space model input parameter vector
$\boldsymbol{h}$	state space model observation vector
$\boldsymbol{I}$	the identity matrix
i	arbitrary non-negative integer value
$\boldsymbol{K}_t$	Kalman gain matrix at time step t
$\hat{k}_t$	adaptive gain at time step t
l	lead-time (in time steps) of forecast time step
m	order of the transfer function numerator polynomial
n	order of the transfer function denominator polynomial
$\boldsymbol{P}_t$	Kalman filter state covariance matrix at time step t
$\boldsymbol{Q}$	state space model noise variance ratio matrix
q	adaptive gain noise variance ratio
R_l^2	coefficient of determination at lead-time l
R_T^2	coefficient of determination (simulation)
r_t	observed catchment average rainfall at time step t
s_t	variance ratio of the estimate of the adaptive gain at time step t
t	time step index number
t_0	time step at which a forecast is made (forecast origin)
u_t	catchment average effective rainfall at time step t
v_t	value of arbitrary variable at time step t
$\hat{\boldsymbol{x}}_t$	state space model state vector estimate at time step t
$\hat{\boldsymbol{x}}_{t+l\|t}$	forecast state vector at lead-time l time steps ahead, made at time step t
y_t	gauged instantaneous catchment discharge at time step t
$\hat{y}_t$	estimated instantaneous catchment discharge at time step t
$\hat{y}_{t+l\|t}$	forecast instantaneous catchment discharge at lead-time l time steps ahead, made at time step t
$z^{-\mathrm{i}}$	backward shift operator, defined such that $z^{-\mathrm{i}}\, v_t = v_{t-i}$
α	order of auto-regressive error prediction model
γ	exponent coefficient in exponential effective rainfall function
δ	catchment lag (number of time steps)
$\hat{\varepsilon}_{t+l\|t}$	estimated difference between deterministic model flow forecast and observed flow at lead-time l time steps ahead, with forecast made at time step t
λ_0	coefficient in the Kalman filter adaptive variance relationship
λ_1	coefficient in the Kalman filter adaptive variance relationship
$\hat{\sigma}_t^2$	state space model observation noise variance estimate at time t
φ_i	auto-regressive model parameters
ω	exponent in power law effective rainfall function

1. Introduction

In general, operational fluvial flood forecasting systems require cascades of rainfall, rainfall–runoff, channel-flow routing and storm-surge models. In practice, some of these model types can be omitted (Lettenmaier and Wood, 1993), but rainfall–runoff models are central to most systems, either for generating the required forecasts directly or for providing inflow forecasts for channel-flow routing models. Real-time updating algorithms that adjust model predictions based upon recent model performance are often employed to improve forecast accuracy (e.g. Beven, 2009; Lettenmaier and Wood, 1993; Moore, 2007; Refsgaard, 1997; Romanowicz *et al.*, 2006).

Lumped conceptual rainfall–runoff (CRR) models (Wheater *et al.*, 1993) are widely used to fulfil the rainfall–runoff modelling requirement of operational flood forecasting systems (e.g. Guo *et al.*, 2004; Moore *et al.*, 1994; Rabufetti and Barbero, 2005; Smith *et al.*, 2003; Vehviläinen *et al.*, 2005; Werner and van Dijk, 2005; Whitfield, 2005). One of the drawbacks of CRR models is that they are often over-parameterised, so that it may not be possible to identify a single, best parameter set for a specific catchment (Beven, 2001). The practical corollary of this is that it can introduce uncertainty into predictions made by the model.

The data-based mechanistic (DBM) modelling approach has been proposed as a means of identifying and calibrating model structures that are not over-parameterised while maintaining a hydrological interpretation of the derived model structure (e.g. Young, 1998, 2006b). In practice, this involves identifying the most appropriate model structure from a fairly general class of models using statistical identification procedures. These procedures exclude unnecessary complexity from the model structure, allowing optimal parameters to be determined objectively. The DBM approach contrasts with the typical application of CRR models where a model structure is chosen subjectively, without reference to catchment-specific data. Although this has the potential benefit of including hydrological process understanding in the model, it also introduces the potential for making incorrect prior assumptions and for selecting an over-parameterised model structure, which may result in sub-optimal model performance. The recent development of CRR modelling toolkits that facilitate comparison of alternate CRR structural components goes some way to ameliorating this issue (Moore, 2007; Wagener *et al.*, 2002), but these have not yet been adopted widely in practice and tend to be based on a relatively limited set of components. Despite these differences, there are parallels between the two approaches, and similarities and overlaps between the structural forms of the models used.

The DBM approach has been applied to rainfall–runoff modelling (Lees, 2000; McIntyre and Marshall, 2010; Young, 2003; Young and Beven, 1994) and lends itself naturally to the incorporation of real-time updating for flood forecasting applications (Leedal *et al.*, 2009; Lees *et al.*, 1994; Romanowicz *et al.*, 2006; Young, 2002, 2007; Young and Tomlin, 2000). These published studies have shown that the approach has promise for real-time flood forecasting, but most have applied the methodology to upland UK catchments using hourly observed data. However, lowland UK catchments are of considerable practical interest as they experience substantial anthropogenic pressure (Wheater and Peach, 2004) and may require alternative model formulations due to different hydrological controls and the greater influence of groundwater (Bell *et al.*, 2009). Furthermore, the identification algorithms typically used with DBM modelling can experience problems if used with observed data where the data interval is short compared with the timescales of the processes being modelled (Young and Garnier, 2006). Furthermore, they appear not to have been demonstrated to work satisfactorily at catchment scale with the 15 min data commonly used in operational forecasting practice. The forecasting performance of DBM and CRR models also remains to be compared. Consequently, questions remain over the utility of DBM flood forecasting models, which this paper seeks to answer through a number of case studies.

2. DBM rainfall–runoff modelling

Published applications of the DBM approach to rainfall–runoff modelling (Section 1) have been based upon spatially lumped, non-linear, discrete-time (DT), stochastic transfer function models, used to predict the total stream flow and accompanying uncertainty bounds on the prediction. This paper does not, however, calculate or investigate the performance of the uncertainty bounds, as good deterministic ('best estimate') performance is the main requirement in some applications and is a prerequisite for narrow uncertainty ranges in probabilistic forecasting applications.

2.1 The DBM approach

The common formulation of a deterministic DBM rainfall–runoff model is given by a non-linear effective rainfall transformation:

$$u_t = cf(y_t)r_t \tag{1a}$$

where the observed flow acts as a surrogate for catchment wetness (Moore, 1982; Young and Beven, 1994) and a single-input DT linear transfer function

$$\hat{y}_t = \frac{b_0 + b_1 z^{-1} + b_2 z^{-2} + \cdots + b_m z^{-m}}{1 + a_1 z^{-1} + a_2 z^{-2} + \cdots + a_n z^{-n}} u_{t-\delta} \tag{1b}$$

or its equivalent difference equation:

$$\begin{aligned} \hat{y}_t = &- a_1\hat{y}_{t-1} - a_2\hat{y}_{t-2} - \cdots - a_n\hat{y}_{t-n} \\ &+ b_0 u_{t-\delta} + b_1 u_{t-\delta-1} + b_2 u_{t-\delta-2} \\ &+ \cdots + b_m u_{t-\delta-m} \end{aligned} \tag{1c}$$

represents the routing of u to the catchment outlet.

The use of the effective rainfall transformation (Equation 1a), rather than the explicit soil moisture accounting procedures used with CRR models, is a notable difference between the two approaches.

Identification and calibration of a DBM model may be treated as a three-stage process. The first stage is to identify the structure of the linear transfer function (the values of n, m and δ), for which

various methodologies could be used (e.g. Box *et al.*, 2008). However, most previously published applications of DBM modelling have identified the model structure by fitting a number of possible structures to the calibration dataset, assuming $u_t = r_t$, and selecting the most appropriate; this approach has been followed here. The simplified, refined instrumental variable (SRIV) algorithm (Young, 1984) is often used for fitting the model to the data, while the suitability of each structure is measured by the simulation mode coefficient of determination (R_T^2) and the Young information criterion (YIC) (Lees, 2000). The coefficient of determination is similar to the Nash–Sutcliffe efficiency (Nash and Sutcliffe, 1970) and is a measure of how well the model explains the observed data, while the YIC is a heuristic measure that attempts to trade-off performance against over parameterisation. The selected model structure is denoted by the triad ($n\ m{+}1\ \delta$) (Lees, 2000).

Once the structure of the transfer function has been estimated, the form of $f(.)$ can be identified non-parametrically through state-dependent parameter (SDP) analysis (Young *et al.*, 2001). This is achieved by using a recursive smoothing algorithm to generate time-variable estimates of the parameters of the linear transfer function (usually in a simplified reduced-order form), after first sorting the calibration data according to the observed flow. The parameter estimates are then plotted graphically against the corresponding values of the observed flow to reveal the relationships between them. Assuming that there is little variation in the transfer function denominator parameters, and a common relationship between the numerator parameters and the observed flow can be found and factored out, an appropriate parameterisation of the relationship is then chosen. This often takes the form of a power law (Young, 2002):

$$\text{2a.} \quad f(y_t) = y_t^{\omega}$$

or a negative exponential function (Young, 2006a):

$$\text{2b.} \quad f(y_t) = 1 - \exp(-\gamma y_t)$$

Separating the structural identification of the linear and non-linear components in this way does not appear to have been justified theoretically, but seems to work satisfactorily in practice (see references in Section 1). It may be considered reasonable, however, as the non-linearity only affects the magnitude, not the timing, of the response to rainfall.

Finally, the parameters ($a_1 \ldots a_n,\ b_0 \ldots b_n$) of the linear transfer function are jointly optimised with the parameters of the non-linear model, using a suitable non-linear optimisation algorithm and the SRIV algorithm (or similar) for the transfer function parameters. The scaling factor c is not generally optimised, but calculated from mass balance or a constraint on peak rainfall (e.g. Ratto *et al.*, 2007; Young, 2003).

Once calibrated, the model is interpreted in mechanistic terms, usually through partial fraction decomposition of the transfer function into a number of linear reservoirs connected in parallel or series (Young and Beven, 1994). A commonly occurring decomposition is two linear stores in parallel (Figure 1), which can be mechanistically interpreted as the catchment comprising parallel baseflow and storm-flow paths. If a feasible mechanistic interpretation of the calibrated model cannot be found, the model is rejected and alternative forms sought. Finally, the calibrated model is validated against a dataset not used in its identification (Young, 2006b).

2.2 Real-time flood forecasting formulation

Published applications of the DBM approach to real-time flood forecasting have used several different updating schemes. These fall into two broad categories: parameter updating and state updating (Refsgaard, 1997). Parameter updating is achieved through an adaptive gain mechanism (Lees *et al.*, 1994) and state updating through reformulating the identified DBM model in a stochastic state-space form and setting it within a Kalman filter algorithm (Young and Tomlin, 2000). Neither of these approaches models the temporal dependence structure of the errors, however. The two approaches have also been combined in a number of different formulations (Leedal *et al.*, 2009; Romanowicz *et al.*, 2006; Young, 2002), including the use of a variable observation noise variance in the Kalman filter to account for the heteroscedasticity of the errors in the observed data.

The updating framework applied in this paper is adapted from those previously published. The DBM model is reformulated as a stochastic state-space model, with the elements of the true, but unknown, state vector $\boldsymbol{x}$ being the discharges from each pathway for a parallel pathway model, and the parameter matrix $\boldsymbol{F}$ and the parameter vectors $\boldsymbol{g}$ and $\boldsymbol{h}$ being calculated from the a and b parameters of the identified transfer function model (Romanowicz *et al.*, 2006; Young, 2002). This is then set within a joint Kalman filter–adaptive gain (KF-AG) algorithm to recursively update the model states for time steps prior to the commencement of a forecast (the equations are provided here to give a full description of the method, but a general understanding of the method should be possible by reading only the associated text):

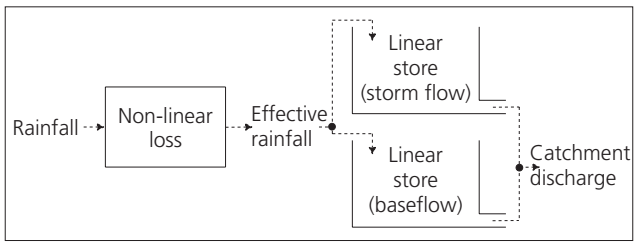

Figure 1. Example conceptual interpretation of a DBM rainfall–runoff model decomposed into two linear stores in parallel (adapted from Young, 2003).

Prediction step:

$$\text{3a.}\quad \hat{\boldsymbol{x}}_t^{(\mathrm{p})} = \boldsymbol{F}\hat{\boldsymbol{x}}_{t-1}^{(\mathrm{c})} + \boldsymbol{g}u_{t-\delta}$$

$$\text{3b.}\quad \hat{y}_t^{(\mathrm{p})} = \boldsymbol{h}\hat{\boldsymbol{x}}_t^{(\mathrm{p})}$$

$$\text{3c.}\quad \hat{\sigma}_t^2 = \lambda_0 + \lambda_1(\hat{y}_t^{(\mathrm{p})})^2$$

$$\text{3d.}\quad \boldsymbol{P}_t^{(\mathrm{p})} = \boldsymbol{F}\boldsymbol{P}_{t-1}^{(\mathrm{c})}\boldsymbol{F}^{\mathrm{T}} + \hat{\sigma}_t^2\boldsymbol{Q}$$

with superscript T representing the matrix transpose and superscripts (c) and (p) denoting results from the Kalman filter correction and prediction steps.

Correction step:

$$\text{3e.}\quad \boldsymbol{K}_t = \boldsymbol{P}_t^{(\mathrm{p})}\boldsymbol{h}^{\mathrm{T}}(\hat{\sigma}_t^2 + \boldsymbol{h}\boldsymbol{P}_t^{(\mathrm{p})}\boldsymbol{h}^{\mathrm{T}})^{-1}$$

$$\text{3f.}\quad \hat{\boldsymbol{x}}_t^{(\mathrm{c})} = \hat{\boldsymbol{x}}_t^{(\mathrm{p})} + \boldsymbol{K}_t(y_t - \hat{y}_t^{(\mathrm{p})})$$

$$\text{3g.}\quad \boldsymbol{P}_t^{(\mathrm{c})} = (\boldsymbol{I} - \boldsymbol{K}_t\boldsymbol{h})\boldsymbol{P}_t^{(\mathrm{p})}$$

$$\text{3h.}\quad \hat{y}_t^{(\mathrm{c})} = \boldsymbol{h}\hat{\boldsymbol{x}}_t^{(\mathrm{c})}$$

Update adaptive gain:

$$\text{3i.}\quad s_t^{(\mathrm{p})} = s_{t-1}^{(\mathrm{c})} + q$$

$$\text{3j.}\quad s_t^{(\mathrm{c})} = s_t^{(\mathrm{p})} - (s_t^{(\mathrm{p})}\hat{y}_t^{(\mathrm{c})})^2[1 + s_t^{(\mathrm{p})}(\hat{y}_t^{(\mathrm{c})})^2]^{-1}$$

$$\text{3k.}\quad \hat{k}_t = \hat{k}_{t-1} + s_t^{(\mathrm{c})}\hat{y}_t^{(\mathrm{c})}(y_t - \hat{k}_{t-1}\hat{y}_t^{(\mathrm{c})})$$

Filtered flow estimate:

$$\text{3l.}\quad \hat{y}_t = \hat{k}_t\hat{y}_t^{(\mathrm{c})}$$

The prediction step of the Kalman filter uses the prediction form of the stochastic state-space model (Equations 3a and 3b) to predict the states and the total discharge at a time step for which observed data are available, based upon the previously estimated states and the rainfall inputs. Equation 3d estimates the variances and covariances of the states, which indicate the uncertainty of the estimate of the state vector.

The Kalman filter correction step then updates the state estimate (Equation 3f) by an amount that depends upon the difference between the predicted and observed flow at the time step, weighted to account for their relative uncertainties. To account for the heteroscedastic error structure of the observed flows, the variance of the observed flow is increased with flow magnitude (Equation 3c). This variance is estimated from the predicted flow, rather than the observed flow, to allow it to be estimated in the forecast period to give an estimate of the uncertainty of the forecast, although this is not required for the work reported here. The variances and covariances of the updated states are also revised (Equation 3g). The adaptive gain, which is simply a multiplier on the filtered flow estimate (Equation 3l), is then estimated (Equation 3k) using an independent Kalman filter.

Forecasts are made by applying the state-space model prediction equations recursively at each forecast lead-time l up to the maximum possible lead-time (restricted to δ time steps due to the need to use the observed flow from δ time steps before the predicted flow in the calculation of the effective rainfall) without any ensuing correction step:

Forecast step:

$$\text{4a.}\quad \hat{\boldsymbol{x}}_{t_0+l|t_0} = \boldsymbol{F}\hat{\boldsymbol{x}}_{t_0+l-1|t_0} + \boldsymbol{g}u_{t_0+l-\delta}$$

$$\text{4b.}\quad \hat{y}_{t_0+l|t_0} = \hat{k}_{t_0}\boldsymbol{h}\hat{\boldsymbol{x}}_{t_0+l|t_0}$$

The initial condition for the forecast is provided by the updated state vector at the forecast origin time t_0 and the gain is held constant at its estimate at t_0.

The KF-AG algorithm introduces a number of hyperparameters that control its behaviour. These are: λ_0 and λ_1, the coefficients of the heteroscedastic observation noise equation; q, the noise variance ratio (NVR) of the adaptive gain; and the elements of the NVR matrix of the Kalman filter, $\boldsymbol{Q}$. The NVR matrix is usually assumed to be diagonal (Young and Tomlin, 2000), in which case it introduces one hyperparameter for each of the parallel flow

paths. These hyperparameters may be calibrated automatically using a non-linear optimisation algorithm to give the optimal forecast performance at a chosen lead-time (Young, 2002).

2.3 Continuous-time DBM model identification

An alternative approach to linear transfer function model identification has been recommended by Young (2004) and applied to rainfall–runoff simulation modelling by Young (2004) and Ratto *et al.* (2007). In this approach, the transfer function is defined and identified in a continuous-time (CT) form, again described by the triad (n m+1 δ). Fitting CT models follows the same procedure as described in Section 2.1, but with a modified version of the SRIV (or similar) algorithm to account for the CT formulation (Young and Garnier, 2006). The potential advantage of the CT approach is that it is less susceptible to problems when fitting models to data where the interval between observations is short compared with the timescales of the system being modelled (Young and Garnier, 2006) and hence may be preferable for 15 min data. The identified CT model can then be converted to a discretely coincident DT form (O'Connor, 1982; Young *et al.*, 2006) and recast into the KF-AG updating framework for forecasting.

3. CRR modelling for flood forecasting

Many different CRR models have been used for real-time flood forecasting and it would be impractical to compare even a significant sample of them with DBM models. The simplifying approach taken in this paper is to compare the DBM results with those of a single CRR model. The most commonly used form of the probability distributed model (PDM) (Moore, 2007; Moore *et al.*, 2005) was selected for this purpose as it gives reasonably good forecasting performance across a range of catchments (Moore *et al.*, 2000) and hence may be indicative of the flood forecasting performance attainable with CRR models.

3.1 The probability distributed model

The PDM used in this study is a 12-parameter, lumped CRR model that conceptualises the catchment as a soil, groundwater and two (serially connected) surface water stores. All rainfall enters the catchment through the soil store. Water can leave the soil store by evaporation, drainage to the groundwater store or rapid runoff to the first surface store. Catchment discharge is calculated as the sum of the outflows from the groundwater and second surface water stores. The soil store represents the spatial variability of storage capacity with a three-parameter Pareto distribution, with only the saturated proportion contributing rapid runoff to the surface water stores. Drainage occurs at a rate related to the total soil storage, however. The groundwater store is modelled as a cubic reservoir and the surface stores as linear reservoirs.

The model has inputs of rainfall and potential evaporation, and ideally requires long periods of data, typically 5 years, for calibration, and more for validation. Observed potential evaporation data were not available, so a sine curve was used to estimate daily potential evaporation (Bell and Moore, 1998) based on a UK average rate of 1·5 mm/day and a minimum of zero in mid-winter (Calder *et al.*, 1983). For the purposes of this study, the 12-parameter PDM was implemented in Matlab®.

3.2 Real-time updating of the PDM

A range of real-time updating approaches could be used with the PDM. State updating could be achieved using either the empirical scheme derived by Moore (2007) or by reformulating the model in a stochastic filtering framework similar to the Kalman filter component of the KF-AG algorithm used with the DBM model. This latter approach would require the use of a non-linear filter, however, such as the extended Kalman filter (e.g. Georgakakos, 1986; Refsgaard, 1997) or the ensemble Kalman filter (e.g. Weerts and El Serafy, 2006). Alternatively, the adaptive gain component of the KF-AG algorithm could be used to provide a simple form of parameter updating (e.g. Lees *et al.*, 1994). Error prediction is also possible using, for example, an auto-regressive moving-average (ARMA) model (e.g. Moore, 2007) to predict the differences between the simulated and observed flows in the forecast period. These predicted errors are then added to the predictions from the CRR model to give the updated flow forecasts.

An error prediction scheme was chosen for this study as this approach is widely used in practice and can be applied to any conceptual or time-series model, and so is considered better for the comparative work described in this paper. Moore (2007) notes that a third-order auto-regressive (AR) model is often sufficient, so the implemented scheme was constrained to use an AR model:

$$\hat{\varepsilon}_{t_0+l|t_0} = \varphi_1 \hat{\varepsilon}_{t_0+l-1|t_0} + \varphi_2 \hat{\varepsilon}_{t_0+l-2|t_0} + \cdots + \varphi_\alpha \hat{\varepsilon}_{t_0+l-\alpha|t_0} \quad 5.$$

rather than an ARMA model. Equation 5 is applied recursively to predict the errors through the forecast period, with the observed errors being used as initial conditions.

Application of the AR error correction scheme requires the order α to be identified and the parameters φ to be calibrated. One approach to identifying the order is to fit models for a range of orders and select based on the value of the Akaike information criterion (AIC) (Akaike, 1974). The AIC measures the performance of the model, but with a penalty for additional parameters, so striking a balance between calibration performance and over parameterisation. AR models of order α are denoted as AR(α) models.

4. Case study catchments

Two catchments in south-east England, the River Lod at Halfway Bridge and the River Wallington at North Fareham (Table 1), were selected for the case studies. These catchments were chosen as being relatively natural, while having different geomorphologi-

	River Lod at Halfway Bridge	River Wallington at North Fareham
Catchment area: km^2	52	111
BFIHost*	0·48	0·64
Maximum elevation: mAOD†	274	248
Station elevation: mAOD	14	4
QMED: m^3/s‡	16·4	17·8
QMED: mm/h	1·135	0·577

* Catchment baseflow index derived from the HOST soil classification
† Metres above Ordnance Datum
‡ Median value of the instantaneous annual maximum discharge series

Table 1. Descriptive statistics for the case study catchments (CEH, 2010; EA, 2010)

cal settings and relatively long flow and tipping-bucket rain gauge (TBR) records of reasonable quality.

The River Lod is a tributary of the River Rother in West Sussex. The catchment comprises a mix of sands and clay and is notably steep in the upper part of the catchment. Although relatively natural, flows are influenced by mill operation in the lower flow range. There are two TBRs just outside the catchment (Northchapel and Iping Mill), from which catchment average rainfall was estimated using Thiessen polygons.

The Wallington catchment is located in south-east Hampshire. It comprises sands and clays in the lower part of the catchment, but chalk in the upper part of the catchment. Catchment average rainfall was again estimated from one TBR within the catchment (Worlds End) and another just outside the catchment (Cowplain) using Thiessen polygons.

5. Model identification and simulation performance

This section describes the identification and calibration of the DT DBM models, the calibration of the CRR models and the validation of their performance as simulation models using independent test datasets.

5.1 DBM model identification and calibration

DT DBM models were fitted to 4–5 year periods of 15 min data for each catchment (Table 2). These datasets are significantly longer than have been used in previous studies (e.g. Lees, 2000; McIntyre and Marshall, 2010; Young, 2003; Young and Beven, 1994), but allow a more robust performance assessment and comparison with the CRR model.

Linear transfer function structures were first identified for each catchment from the calibration datasets using the SRIV algorithm from the Captain toolbox for Matlab (LU, 2011; Taylor *et al.*, 2007), yielding (2 2 27) structures for both catchments. Preliminary investigation applying SDP analysis to short data periods had indicated that the negative exponential form of non-linearity (Equation 2b) was most suitable for these catchments, so this form was adopted for both catchments without carrying out SDP analysis on the full calibration datasets. This approach was taken because the direct application of standard forms of non-linearity is likely to be a more pragmatic approach than SDP analysis of every catchment in any widespread application of DBM modelling to operational forecasting. The parameters of these non-linear models were optimised using a simplex algorithm and the sum of squared errors as the objective function. Nested within this algorithm, the linear transfer function was optimised using the SRIV algorithm to ensure that the optimal combination of non-linear and linear parameters was found. The optimum parameter sets for both catchments gave satisfactory performance and had mechanistic interpretations of two linear stores in parallel (Table 2).

	River Lod at Halfway Bridge		River Wallington at North Fareham	
Dataset				
Calibration period start	01/07/02 21:00		07/08/03 00:00	
Calibration period end	30/03/07 10:45		30/06/08 23:45	
Maximum flow: mm/h	0·962		0·521	
Maximum flow/QMED	0·85		0·90	
Minimum flow: mm/h	0·002		0·0003	
	Structure	R_T^2	Structure	R_T^2
Performance				
DT DBM	(2 2 27)	0·82	(2 2 27)	0·85
CRR	(PDM)	0·69	(PDM)	0·62
CT-identified DBM	(2 2 17)	0·88	(2 2 25)	0·82

Table 2. Calibration datasets and performance

5.2 Conceptual rainfall–runoff model calibration

PDM CRR models were calibrated for the Lod and Wallington catchments using the same datasets as for the DT DBM models. Calibration was carried out using a manual trial-and-error approach, as is common practice operationally, without any supporting automatic optimisation. This may not have found the statistically optimal parameter set and led to poorer statistical fits than for the DBM models (Table 2) but was judged to offer an appropriate compromise between overall fit, performance on peak events and internal behaviour of the model. To achieve adequate performance for the Wallington catchment, the rainfall input had to be reduced significantly to prevent too much water entering the model. Physically, this is thought to be compensating for a catchment water balance that is not closed due to the presence of chalk in the catchment. An alternative approach, therefore, would have been to use a conceptual model that explicitly represents subsurface outflows (e.g. Moore and Bell, 2002), but this was beyond the scope of the present study.

5.3 Simulation model performance

The simulation performance of the DBM models was tested using independent validation datasets of similar lengths to the calibration datasets (Table 3), but which included peak inflows that were substantially higher than those encountered during calibration. For the Lod catchment, it was not possible to have a sufficiently long single validation period due to periods of missing data, so two shorter periods were used.

Preliminary investigation, involving fitting and validating DT DBM models to datasets of similar lengths to those used in previously published studies, had produced validation values of 0·83 (Lod) and 0·88 (Wallington). These values are within the ranges reported by other published studies, which gave confidence in the applicability of the approach to the case study catchments. The performances of the DT DBM models for the full, multi-year calibration and validation datasets reported here (Table 3) are, however, a little worse than for other published studies. This is likely to be due to the much greater degree of extrapolation outside the calibration range in these longer datasets. The CRR model had comparable performance to the DT DBM models for the Wallington catchment, and, in the second data period, for the Lod catchment, (Table 3), despite a significantly poorer fit in calibration. Figure 2 shows example hydrographs from the models for the Wallington catchment for a 10 day sub-period of the validation dataset.

The simulation of the peaks is less satisfactory than the overall fit,

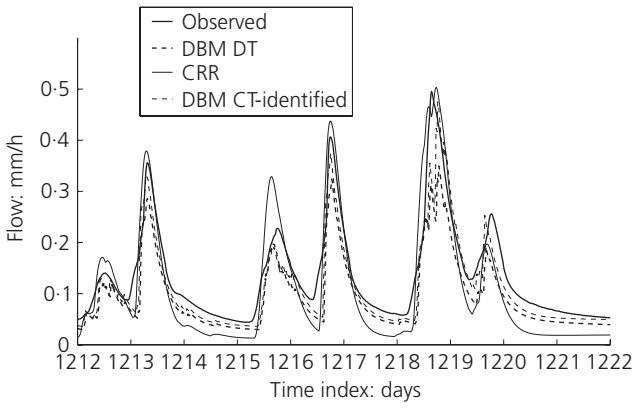

Figure 2. Example simulated hydrographs for the Wallington catchment at North Fareham (validation; observed data within calibration range)

	River Lod at Halfway Bridge (dataset 1)		River Lod at Halfway Bridge (dataset 2)		River Wallington at North Fareham	
Dataset						
Validation period start	23/04/01 20:45		03/04/07 09:30		01/09/99 00:00	
Validation period end	28/06/02 16:45		19/08/09 18:45		30/06/03 23:45	
Maximum flow: mm/h	1·426		2·596		1·619	
Maximum flow/QMED	1·26		2·29		2·81	
Ratio of maximum flows in validation and calibration	1·48		2·70		3·11	
Minimum flow: mm/h	0·004		0·000		0·001	
	Structure	R_T^2	Structure	R_T^2	Structure	R_T^2
Performance						
DT DBM	(2 2 27)	0·81	(2 2 27)	0·76	(2 2 27)	0·76
CRR	(PDM)	0·68	(PDM)	0·74	(PDM)	0·77
CT-identified DBM	(2 2 17)	0·84	(2 2 17)	0·81	(2 2 25)	0·84

Table 3. Validation datasets and performance

with consistent underprediction of the peaks above the calibration range for both the DT DBM and CRR models (Figures 3(a) and 3(b)), which is in accordance with previous studies (Gan and Burges, 1990a, 1990b; Seibert, 2003). This behaviour is particularly marked for the DT DBM model of the Wallington catchment, although much less so for the DT DBM model for the Lod. The degree of underprediction also tends to increase with the magnitude of the peak. The timing errors of the simulated peaks (Figures 3(c) and 3(d)) show substantial scatter and some tendency towards increasing lateness as the peak magnitude increases.

6. Forecasting performance

This section describes the use of real-time updating algorithms with the models and their application to forecasting for the case study catchments.

6.1 Real-time data assimilation formulations

The DT DBM models were recast into the KF-AG updating framework (Equations 3 and 4) and the hyperparameters for each model were jointly optimised on the calibration datasets using the shuffled complex evolution algorithm (Duan *et al.*, 1992). In each case, the hyperparameters were optimised by minimising the sum of squared errors of the forecast at the maximum lead-time possible for that model (i.e. δ in the model structure).

AR error models were identified and fitted to both CRR models, based upon the AIC criterion, using the whole of their respective calibration datasets. An AR(4) model was identified for Lod and an AR(5) for Wallington.

6.2 Forecasting performance comparison

The forecasting performance of each model was assessed by applying it to its validation dataset as an independent performance test; Figure 4 shows example forecast hydrographs. For the assessment, forecasts were generated using each 15 min data point as a forecast origin time and assessed using a number of different metrics.

6.2.1 Lead-time coefficient of determination

The lead-time coefficient of determination is defined as:

$$R_l^2 = 1 - \frac{\mathrm{var}(\hat{y}_{t+l|t} - y_{t+l})}{\mathrm{var}(y_{t+l})} \quad 6.$$

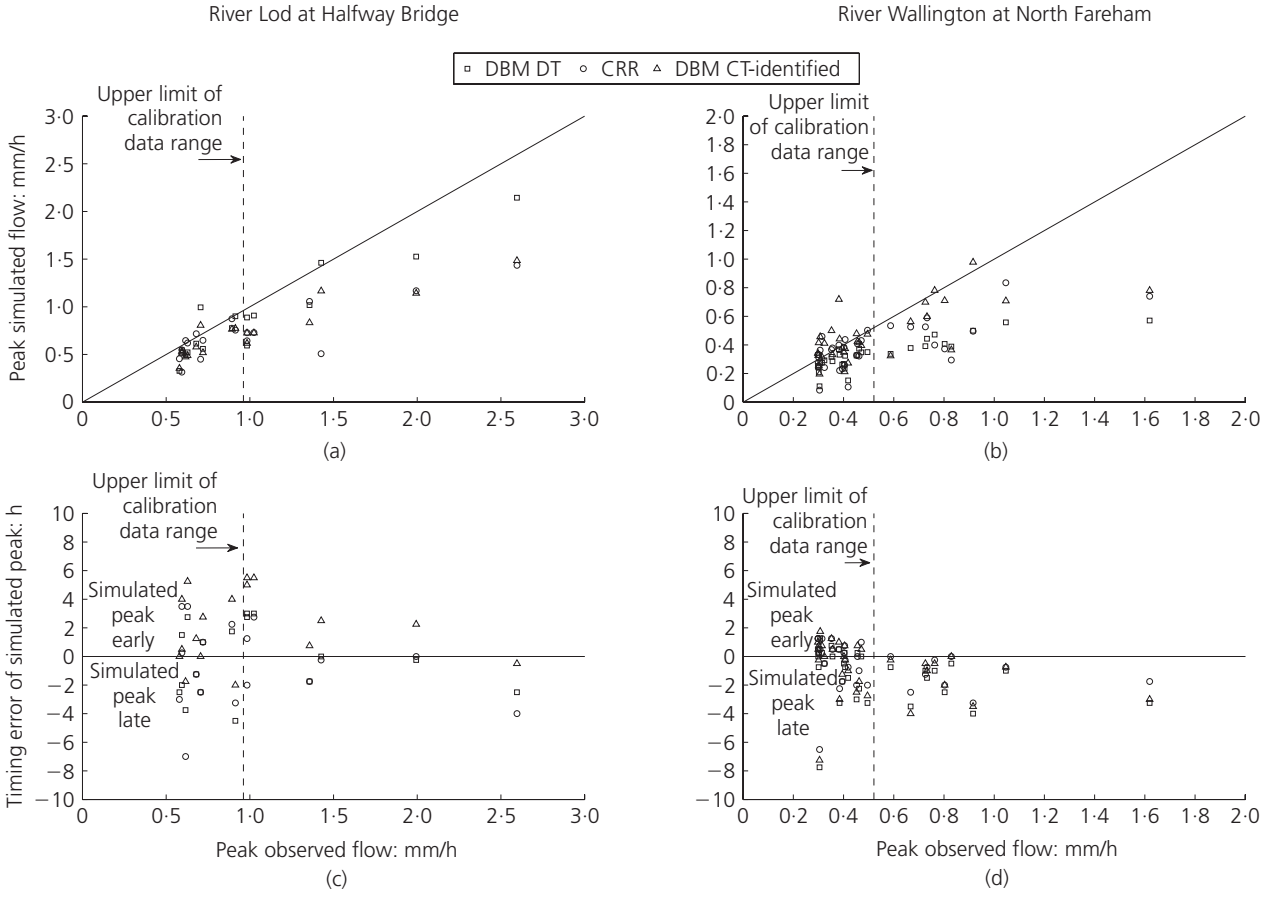

Figure 3. Comparison of the magnitude and timing of the simulations of observed peaks of greater than 0·5 × QMED (validation)

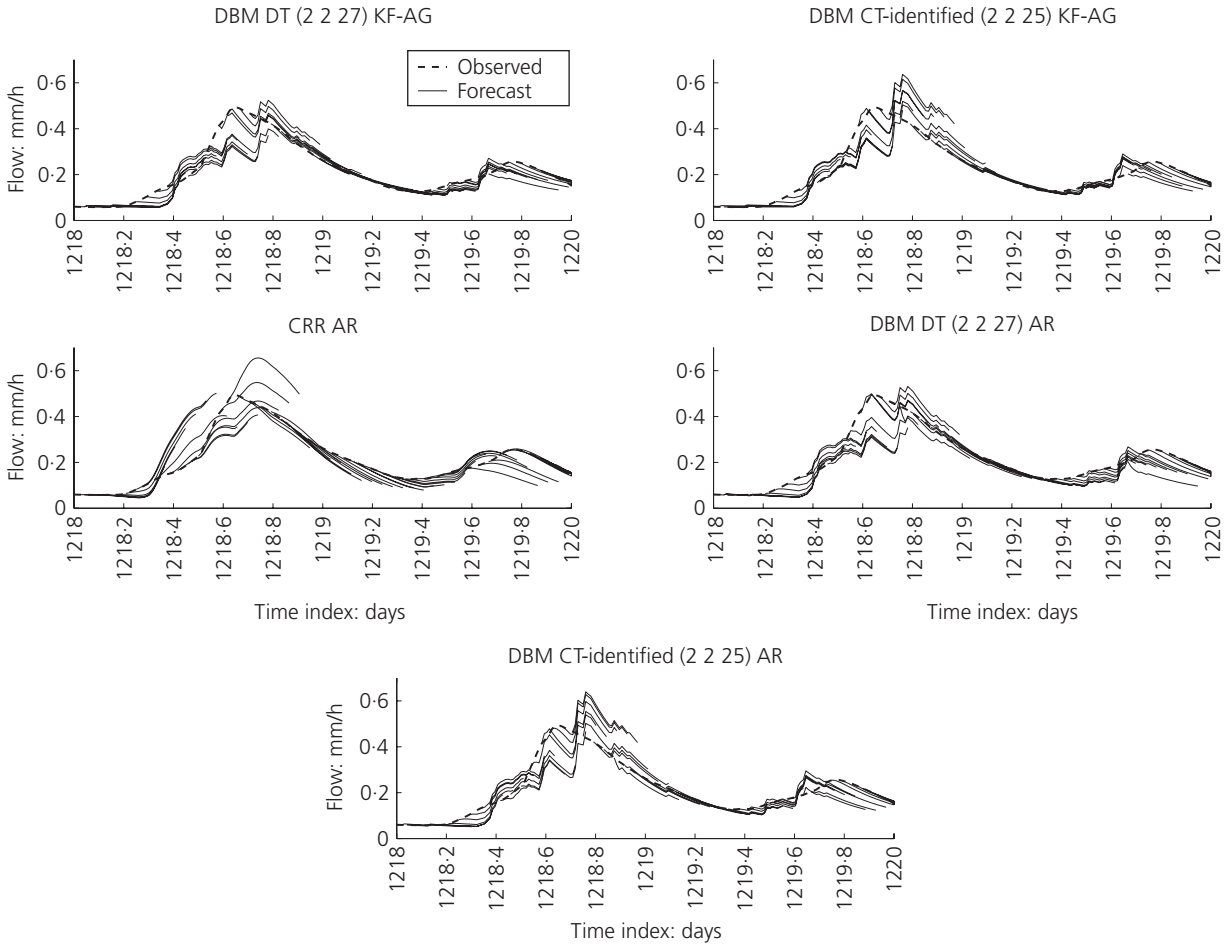

Figure 4. Example forecast hydrographs for each forecasting method for the Wallington catchment at North Fareham (validation; observed data within calibration range). For clarity, forecasts with origin times at 1 h intervals are shown

with its maximum value of 1 indicating a perfect forecast.

For the DT DBM models, the variation of R_l^2 with lead-time (Figures 5 and 6) is comparable to published results (Young, 2002; Young and Tomlin, 2000) and shows that good overall agreement between the forecasts and the observations is achievable. On this measure, the CRR model outperforms the DT DBM models for both catchments, albeit by a relatively small margin, except for longer lead-times on the Lod catchment.

6.2.2 Lead-time quantiles of the percentage errors for consequential forecasts

For forecasts designated as consequential, the percentage errors are calculated as:

$$\frac{\hat{y}_{t_0+l|t_0} - y_{t_0+l}}{y_{t_0+l}} \times 100\% \quad (7)$$

In this study, consequential forecasts are defined as those forecasts with at least one value greater than $0{\cdot}5 \times$ QMED (QMED is the median value of the instantaneous annual maximum discharge series) to exclude forecasts that would be considered trivial in operational use from the analysis.

The 5, 50 and 95% quantiles of the percentage errors for the consequential forecasts for different lead-times (Figure 7) show the CRR models having a narrower spread of errors at shorter lead-times and the DT DBM models having a narrower spread at longer lead-times. The 50% quantile for the CRR model is closer to zero than for the DT DBM, except at longer lead-times for the Wallington catchment, indicating that the CRR model has less tendency to over or underestimate.

6.2.3 Lead-time threshold crossing

The ability to forecast threshold crossings is commonly measured by the probability of detection (POD) and false alarm ratio (FAR). POD is defined as the proportion of observed threshold

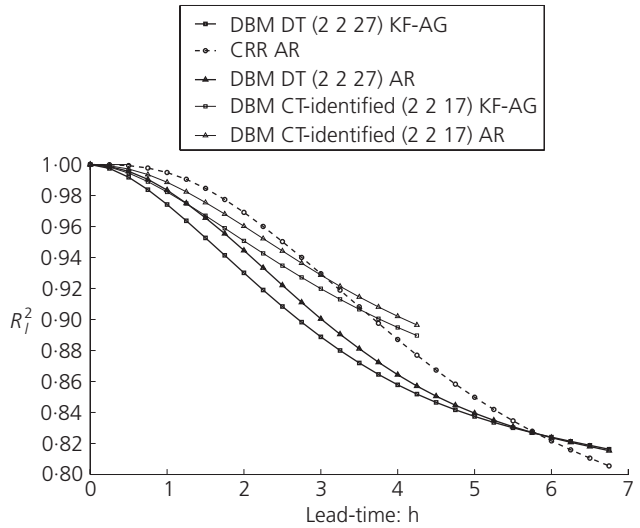

Figure 5. Validation of lead-time forecasting performance for the Lod catchment at Halfway Bridge

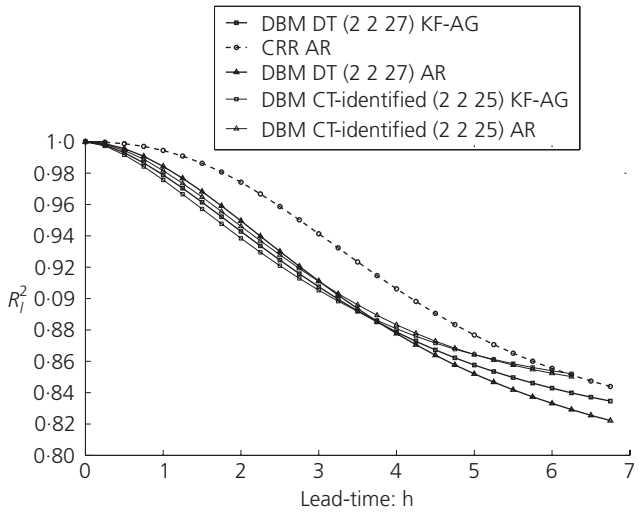

Figure 6. Validation of lead-time forecasting performance for the Wallington catchment at North Fareham

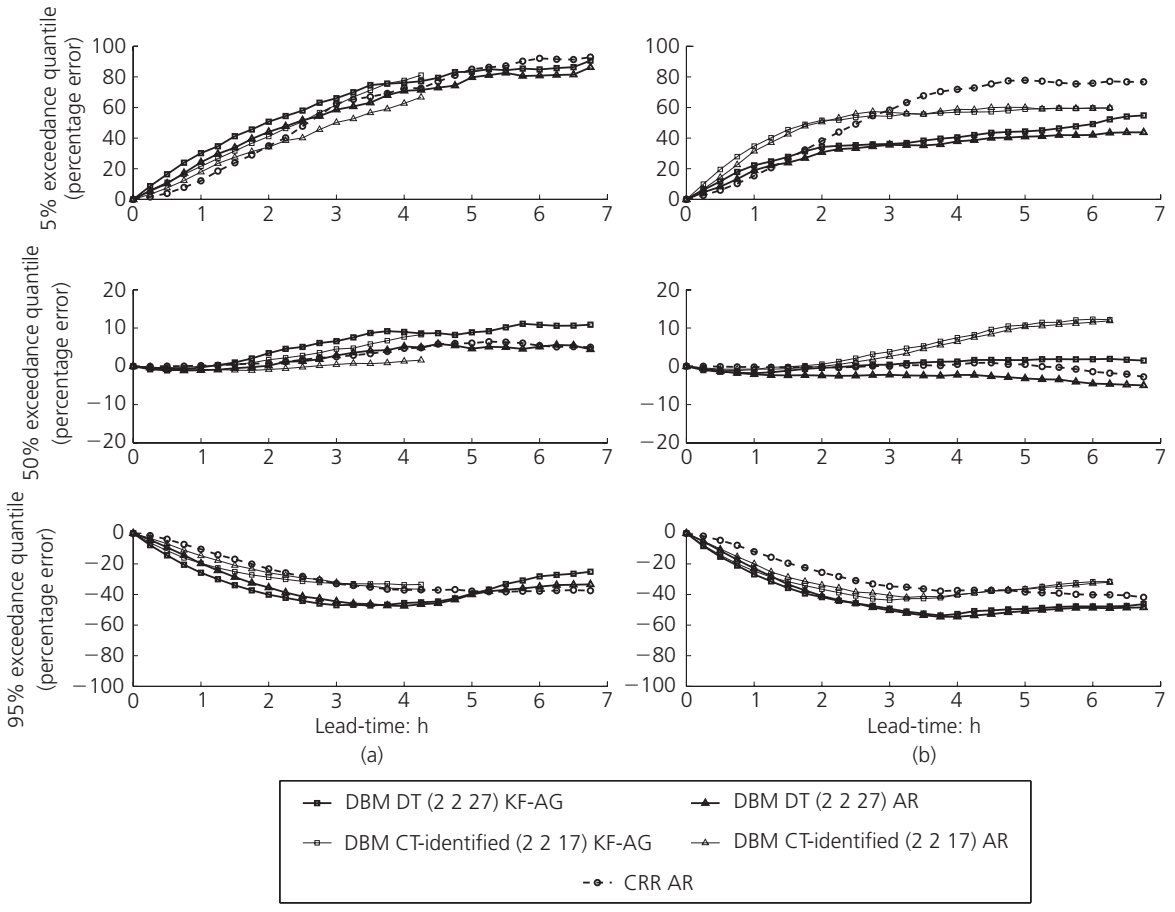

Figure 7. Exceedance quantiles of the errors in the consequential forecasts for (a) River Lod at Halfway Bridge and (b) River Wallington at North Fareham (validation)

crossings that were forecast and FAR as the proportion of forecast threshold crossings that were not followed by an observed threshold crossing. Both measures have the range [0, 1], with 1 being a perfect score for POD and 0 being perfect for FAR.

For these case studies, the thresholds were defined as multiples of QMED. To count as a successful detection, a forecast threshold crossing had to occur no earlier than 3 h before an observed crossing and no later than 1·5 h after the observed crossing. These asymmetric limits were used because, in an operational context, a forecast of a threshold crossing time that is earlier than the observed threshold crossing time is less problematic than a forecast of a threshold crossing time that is later than the observed threshold crossing time.

Only the lowest threshold considered (0·5 × QMED), which is within the calibration range of the models, has enough observed threshold crossings to make any general statements about the threshold crossing performance. For this threshold, the CRR models generally out perform the DT DBM models (Figure 8).

6.2.4 Lead-time quantiles of the percentage errors for peak magnitude forecasts

The percentage errors for the forecasts of the magnitude of the observed peaks are calculated using Equation 7, after peaks have been matched allowing for timing differences. For the Lod catchment, Figure 9 shows the CRR model having a greater tendency to underestimate than the DT DBM model, but a narrower spread of errors. This situation is broadly reversed for the Wallington catchment, although the differences are much less pronounced.

7. Alternative DBM modelling approaches

The analysis above has revealed that, overall, CRR models tended to perform better than DT DBM models for both simulation and forecasting, except at longer lead-times. With the aim of identify-

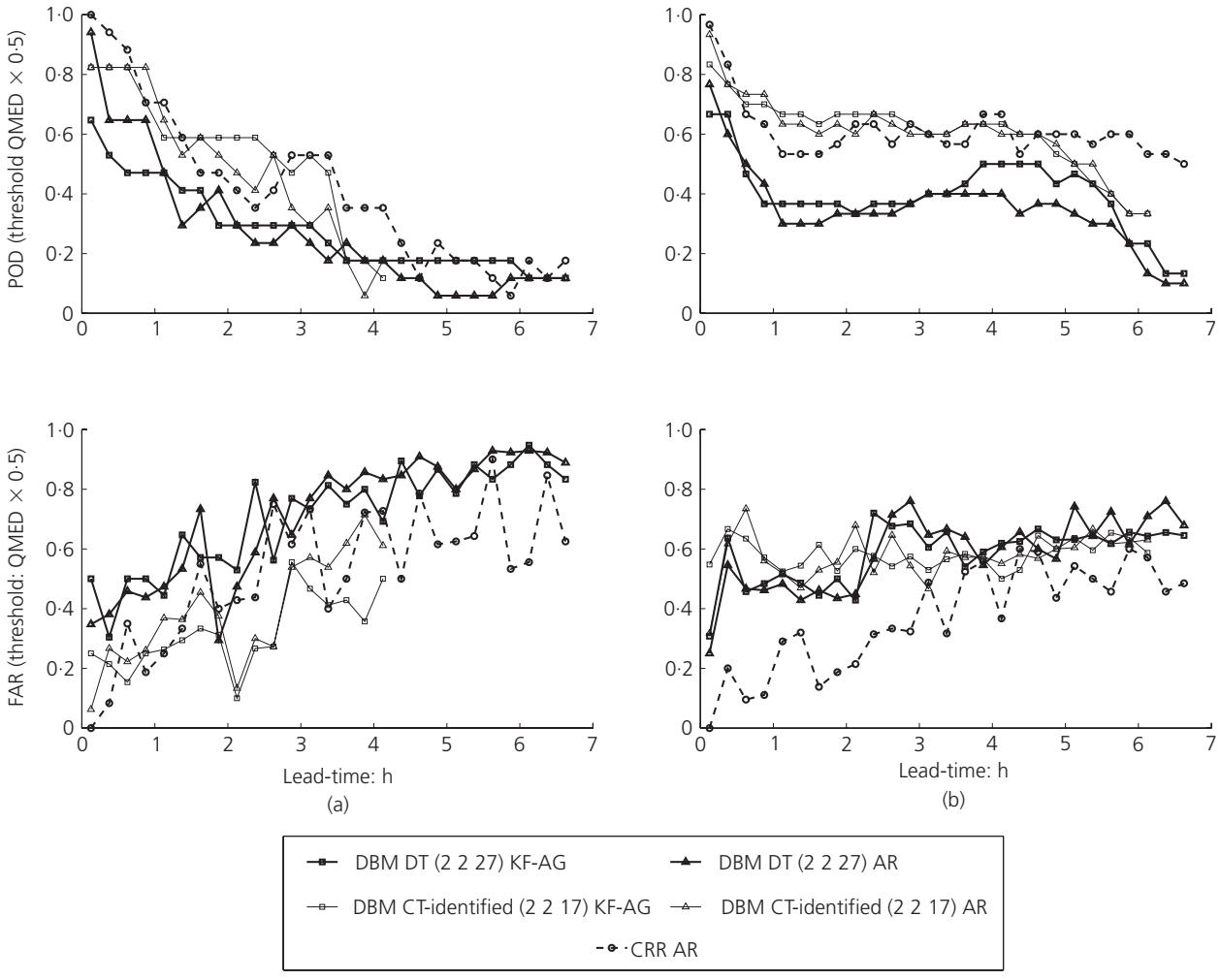

Figure 8. Threshold exceedance forecasting performance for the 0·5 × QMED threshold (validation) for (a) River Lod at Halfway Bridge and (b) River Wallington at North Fareham

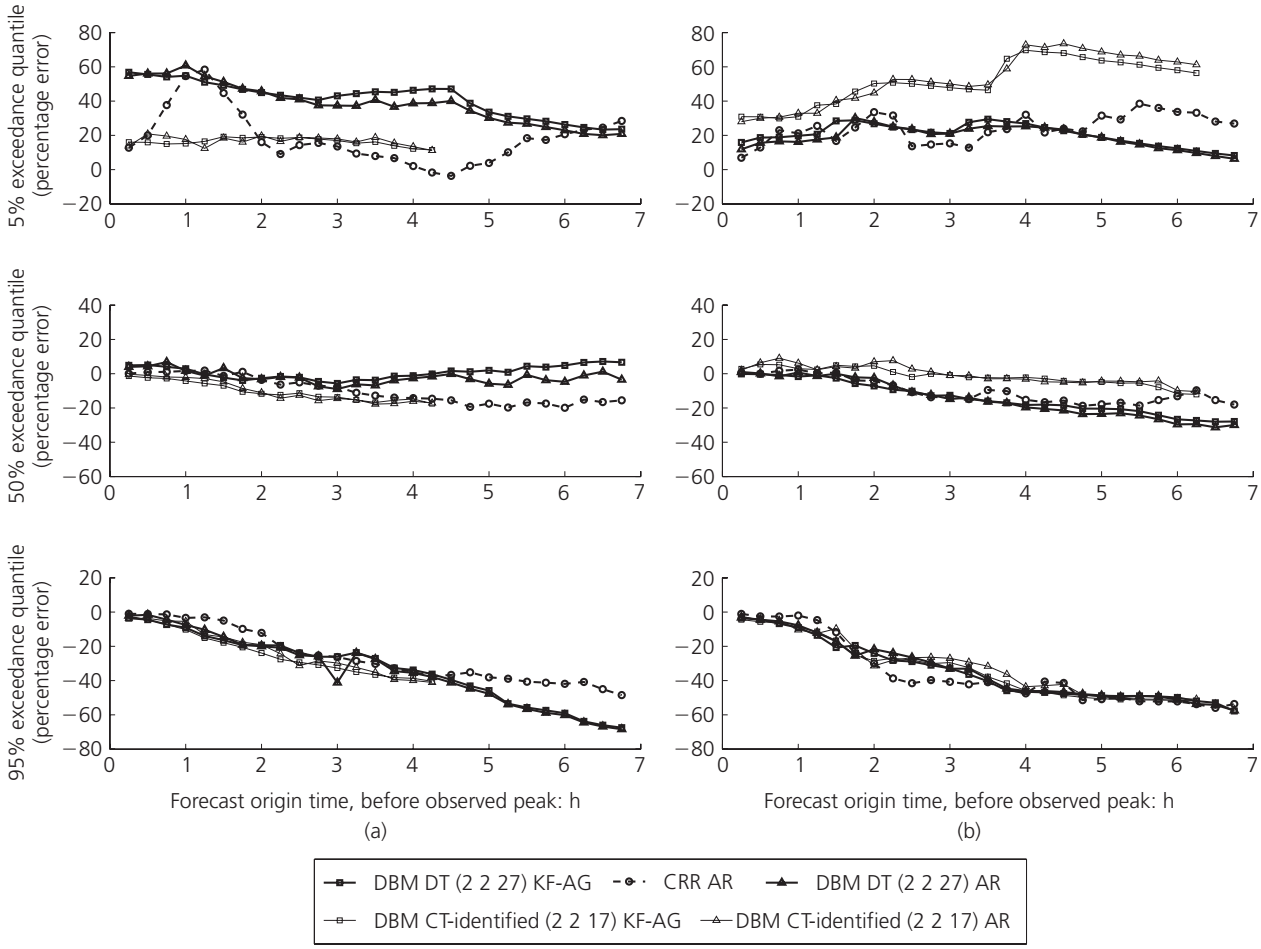

Figure 9. Exceedance quantiles of the errors in the forecasts of observed peaks greater than 0·5 × QMED for (a) River Lod at Halfway Bridge and (b) River Wallington at North Fareham (validation)

ing scope for improvements, this section investigates whether this is due to the underlying DBM model or the real-time updating algorithm.

7.1 Continuous-time DBM model identification

Identification and calibration of CT models for the case study catchments yielded a (2 2 17) model for the Lod and a (2 2 25) model for the Wallington, both with negative exponential non-linearities. These CT models were converted to discretely coincident DT form (Young *et al.*, 2006) for simulation and were found to be able to simulate the overall catchment behaviour better than the previously identified DT models for both catchments in validation (Table 3) and the Lod catchment in calibration (Table 2). The calibration performance for the CT-identified model of the Wallington was only slightly worse than that of the DT model (Table 2). Figure 2 shows an example hydrograph for a period within the calibration range. Figure 3 shows that the CT-identified DBM models have similar difficulties as the other models in extrapolating to peaks beyond the calibration range, although the approach performs better than the other approaches on the Wallington catchment.

7.2 Forecasting performance of the alternative approaches

For forecasting purposes, the discretely coincident DT forms of the CT-identified models were recast into the KF-AG updating algorithm and the hyperparameters optimised on the calibration datasets. AR error prediction models were also fitted to both the original DT and the CT-identified DBM models, as an alternative to the KF-AG algorithm, using the same procedure as used for the CRR model. The performance of these forecasting models was assessed using the same measures and independent validation data as above. Example forecast hydrographs are shown in Figure 4.

The statistical fits of the forecasts (Figures 5 and 6) show the CT-identified models producing overall better forecasts than the original DT models, except for the Wallington catchment where the DT models are a little better at shorter lead-times. The error

quantiles (Figure 7) show the CT-identified model for the Lod catchment having less spread and a lesser tendency to overestimate than the DT model. For the Wallington catchment, however, the spreads of the errors are similar, but the CT-identified model shows a greater tendency to overestimate. The threshold crossing performance of the CT-identified models is better than that of the original DT models (Figure 8), although there is little overall difference in the FAR for the Wallington catchment. There is also little overall difference between the peak forecasting performance of the CT-identified and DT models: the CT-identified model for Lod has less spread (but a greater tendency to underestimate) than the DT model, while this situation is reversed on the Wallington catchment (Figure 9).

The overall fit of the forecasts, as measured by R_T^2 over the range of lead-times, also shows that the AR error prediction resulted in overall better forecasts than the KF-AG algorithm for both the DT and CT-identified DBM models, except at longer lead-times (Figures 5 and 6). This pattern is repeated in the lead-time error quantiles (Figure 7), but not in the lead-time threshold crossing performance, where the KF-AG algorithm gives very marginally better performance overall (Figure 8). The peak error quantiles also show no discernable overall performance difference between the two updating approaches, despite small variations between them (Figure 9). All the performance differences between the AR and KF-AG updating algorithms are relatively small, however, indicating that the underlying model is a greater cause of the performance difference than the real-time updating algorithm.

7.3 CT-identified DBM and CRR forecasting performance

The overall fit of the forecasts (Figures 5 and 6) shows the CRR models generally outperforming the CT-identified DBM models, but the CT-identified models beginning to improve on the CRR performance at longer lead-times. The error quantiles (Figure 7) show the same behaviour, except for an increasing tendency for the CT-identified model to overestimate with lead-time on the Wallington catchment (although the overestimates tend not to be as large as those from the CRR model, so the CT-identified model may be more acceptable). The CT-identified models marginally outperform the CRR models in their threshold crossing performance (Figure 8), although the differences are small, while the peak errors from the CRR models are better constrained than those from the CT-identified models, despite the CT-identified model of the Wallington having a lesser tendency to underestimate (Figure 9).

8. Discussion

The DBM approach to rainfall–runoff modelling offers a number of potential advantages for real-time flood forecasting applications. Model identification and calibration is relatively objective (Young, 2003; Young and Beven, 1994) and faster than manual calibration of a CRR model, and models may be used to forecast stage directly from rainfall without introducing uncertainty due to rating curves (Romanowicz *et al.*, 2006). The principal downside to the approach, using published formulations, is that the maximum forecast lead-time is limited to the length of the natural catchment lag because of the use of observed flow in the effective rainfall calculation (Equation 1a). Although this constraint can be relaxed a little by artificially increasing the lag used, while accepting a reduction in forecast accuracy (Lees *et al.*, 1994), the formulation cannot be used to predict the impact of forecast rainfall. This makes the approach unsuitable for fast-responding catchments with particularly short lag times and longer-term 'outlook' forecasts, both of which are operationally important. An approach to removing this limitation has been demonstrated for simulation modelling (Young, 2003), but its utility for forecasting applications has not yet been established.

The results of this study demonstrate that, relative to previous applications to upland UK catchments using hourly data, the DBM approach is equally suited to rainfall–runoff simulation and forecasting for lowland UK catchments using 15 min data. They also show that CT-identified models may be expected to perform better than, or at least no worse than, DT-identified models across a range of performance measures. This suggests that future research and applications of DBM rainfall–runoff modelling should concentrate on DBM models identified using CT algorithms.

The study has also demonstrated the feasibility of applying CT-identified DBM models in a KF-AG algorithm for real-time forecasting. The results indicate, however, that the use of AR error prediction tends to give better forecasting performance for both DT and CT-identified DBM models than the more commonly used KF-AG algorithm, although the KF-AG algorithm does appear to be a little more effective at longer lead-times. Further development and comparison of updating approaches is therefore required, including KF-AG hyperparameter optimisation schemes and the use of full ARMA error prediction models, as well as combining KF-AG and ARMA approaches. It is likely, however, that the relative performance of the different approaches will be case specific (Refsgaard, 1997).

Comparison of the CRR and DBM results revealed that the CRR model in general gives slightly better forecasting performance than either the DT- or CT-identified DBM models, although not at longer lead-times for some performance measures. This observed difference in forecasting performance can be ascribed to differences in model structure and calibration since the performance difference between a given model with different updating approaches was much smaller than the differences between models. The principal structural differences between the CRR and DBM models are the greater complexity of the runoff generation conceptualisation, non-linearity in the groundwater routing and the variable split of runoff between the quick flow and baseflow paths in the PDM.

For the DBM models, alternative effective rainfall formulations could be determined through more detailed catchment-specific

SDP analysis, possibly modelling the soil moisture dynamics explicitly (e.g. Young, 2003). Alternatively, conceptual runoff generation components could be combined with linear transfer function routing components identified using DBM approaches. Such a hybrid approach would, however, introduce more subjectivity into model identification and care would be needed to maintain the DBM philosophy of deriving the model structure from data to avoid the risk of proliferating the number of 'brand-name' CRR models (Moore *et al.*, 2005). SDP analysis could also be used to identify non-linearities in the routing components (e.g. McIntyre *et al.*, 2011).

Both DBM and CRR model types demonstrated unsatisfactory performance when extrapolating beyond the range of the calibration data. Further investigation is required to identify the extent to which this is due to errors in the input and observed output data used for validation and the extent to which both DBM and CRR model structures and calibration methodologies require improvement. Such improvements may require the incorporation of hydrological process understanding in the model structures, leading to hybrid DBM–CRR models or using DBM methodologies to inform the selection of CRR structural components (e.g. Ratto *et al.*, 2007).

The scope of this study has been relatively limited:

(*a*) it involved only two catchments
(*b*) it placed restrictions on the form of the DBM effective rainfall non-linearity
(*c*) it restricted the routing representation to linear transfer functions
(*d*) the SRIV method of identification may have been replaced by more sophisticated instrumental variable methods.

Furthermore, this study investigated only one CRR model structure, which was calibrated manually and so is unlikely to be optimal. Consequently, further work, using a wider range of model structures and catchments and an improved estimation of potential evaporation, is required to confirm the generality of these findings.

9. Conclusion

This work has shown that discrete-time (DT) DBM models can be applied to lowland UK catchments, using 15 min data, with simulation-mode performance comparable to more complex CRR models and to previously published applications to relatively impermeable catchments using hourly data. However, this simple application of DT DBM models to flood forecasting, including a state and parameter updating scheme, could not generally improve upon the performance of a more complex CRR model, except at the longer lead-times used.

The study has also shown that DBM models identified using continuous-time algorithms can be incorporated into a KF-AG algorithm for real-time forecasting and may perform significantly better than DBM models identified in DT. It has further found that a simple AR error predictor can outperform the more commonly used KF-AG updating algorithm.

Finally, both DBM and CRR models performed unsatisfactorily when extrapolating beyond the range of the calibration data. This is an issue of considerable practical significance and further research is required to understand the causes of this problem and identify solutions.

Acknowledgements

The authors would like to thank the Environment Agency for supporting this work, Qingyun Duan for the Matlab implementation of the SCE-UA algorithm (downloaded from Mathworks (2010)) and the three anonymous reviewers whose comments greatly improved the paper. The Captain toolbox (Taylor *et al.*, 2007) was used under licence from Lancaster University; it can be downloaded (LU, 2011) for use without a licence for 3 months. The views expressed in this paper are those of the authors, and not necessarily those of the Environment Agency.

REFERENCES

Akaike H (1974) A new look at the statistical model identification. *IEEE Transactions on Automatic Control* **19(6)**: 716–723.

Bell VA and Moore RJ (1998) A grid-based distributed flood forecasting model for use with weather radar data: part 2 – case studies. *Hydrology and Earth System Sciences* **2(3)**: 283–298.

Bell VA, Kay AL, Jones RG, Moore RJ and Reynard NS (2009) Use of soil data in a grid-based hydrological model to estimate spatial variation in changing flood risk across the UK. *Journal of Hydrology* **377(3–4)**: 335–350.

Beven KJ (2001) *Rainfall–Runoff Modelling: The Primer*. Wiley, Chichester

Beven KJ (2009) *Environmental Modelling: An Uncertain Future*. Routledge, Abingdon, UK.

Box GEP, Jenkins GM and Reinsel GC (2008) *Time Series Analysis: Forecasting and Control*, 4th edn. Wiley, Chichester.

Calder IR, Harding RJ and Rosier PTW (1983) An objective assessment of soil-moisture deficit models. *Journal of Hydrology* **60(1–4)**: 329–355.

CEH (Centre for Ecology and Hydrology) (2010) www.ceh.ac.uk/data/nrfa (accessed 24/05/2010).

Duan Q, Sorooshian S and Gupta V (1992) Effective and efficient global optimisation for conceptual rainfall–runoff models. *Water Resources Research* **28(4)**: 1015–1031.

EA (Environment Agency) (2010) www.environment-agency.gov.uk/hiflowsuk (accessed 24/05/2010).

Gan TY and Burges SJ (1990a) An assessment of a conceptual rainfall–runoff model's ability to represent the dynamics of small hypothetical catchments 1. Models, model properties, and experimental designs. *Water Resources Research* **26(7)**: 1605–1619.

Gan TY and Burges SJ (1990b) An assessment of a conceptual

rainfall–runoff model's ability to represent the dynamics of small hypothetical catchments 2. Hydrologic responses for normal and extreme rainfall. *Water Resources Research* **26(7)**: 1595–1604.

Georgakakos KP (1986) A generalised stochastic hydrometeorological model for flash-flood forecasting: 1. Formulation. *Water Resources Research* **22(13)**: 2083–2095.

Guo SL, Zhang HG, Chen H *et al.* (2004) A reservoir flood forecasting and control system for China. *Hydrological Sciences Journal-Journal Des Sciences Hydrologiques* **49(6)**: 959–972.

Leedal D, Beven K, Young P, and Romanowicz R (2009) Data assimilation and adaptive real-time forecasting of water levels in the River Eden catchment, UK. In *Flood Risk Management Research and Practice* (Samuels P, *et al.* (eds)). Taylor & Francis, London, pp. 1281–1285.

Lees MJ (2000) Data-based mechanistic modelling and forecasting of hydrological systems. *Journal of Hydroinformatics* **2(1)**: 15–34.

Lees M, Young P, Ferguson S, Beven K and Burns J (1994) An adaptive flood warning scheme for the River Nith at Dumfries. *Proceedings of 2nd International Conference on River Flood Hydraulics* (White WR and Watts J (eds)). Wiley, Chichester, pp. 65–75.

Lettenmaier DP and Wood EF (1993) Hydrologic forecasting. In *Handbook of Hydrology* (Maidment DR (ed.)). McGraw-Hill, New York, pp. 26·1–26·30.

LU (Lancaster University) (2011) www.es.lancs.ac.uk/cres/captain (accessed 19/01/2011).

Mathworks (2010) http://www.mathworks.co.uk/matlabcentral/fileexchange/7671-shuffled-complex-evolution-sce-ua-method (accessed 02/05/2010).

McIntyre N and Marshall M (2010) Identification of rural land management signals in runoff response. *Hydrological Processes* **24(24)**: 3521–3534.

McIntyre N, Young PC, Orellana B, *et al.* (2011) Identification of nonlinearity in rainfall-flow response using data-based mechanistic modelling. *Water Resources Research* **47** w03515, **doi**:10.1029/2010WR009851.

Moore RJ (1982) Transfer functions, noise predictors, and the forecasting of flood events in real-time. In *Statistical Analysis of Rainfall and Runoff* (Singh VP (ed.)). Water Resources Publications, Littleton, CO, pp. 229–250.

Moore RJ (2007) The PDM rainfall–runoff model. *Hydrology and Earth System Sciences* **11(1)**: 483–499.

Moore RJ and Bell VA (2002) Incorporation of groundwater losses and well level data in rainfall–runoff models illustrated using the PDM. *Hydrology and Earth System Sciences* **6(1)**: 25–38.

Moore RJ, Jones DA, Black KB, *et al.* (1994) RFFS and HYRAD: Integrated systems for rainfall and river flow forecasting in real-time and their application in Yorkshire. In *Analytical Techniques for the Development and Operations Planning of Water Resource and Supply Systems, BHS National Meeting, University of Newcastle*. British Hydrological Society, London, Occasional paper 4. See www.hydrology.org.uk/publications/bhs_op4.pdf (accessed 01/12/2011).

Moore RJ, Bell VA and Carrington DS (2000) Intercomparison of rainfal-runoff models for flood forecasting. In *Flood Forecasting: What does Current Research offer the Practitioner? BHS National Meeting, University of Bristol* (Lees M and Walsh P (eds)). British Hydrological Society, London, Occasional paper 12, pp. 69–76. See www.hydrology.org.uk/publications/bhs_op121.pdf (accessed 01/12/2011).

Moore RJ, Bell VA and Jones DA (2005) Forecasting for flood warning. *Comptes Rendus Geoscience* **337(1–2)**: 203–217.

Nash JE and Sutcliffe IV (1970) River flow forecasting through conceptual models part 1 – a discussion of principles. *Journal of Hydrology* **10(3)**: 282–290.

O'Connor KM (1982) Derivation of discretely coincident forms of continuous linear time-invariant models using the transfer function approach. *Journal of Hydrology* **59(1–2)**: 1–48.

Rabufetti D and Barbero S (2005) Operational hydro-meteorological warning and real-time flood forecasting: the Piemonte region case study. *Hydrology and Earth System Sciences* **9(4)**: 457–466.

Ratto M, Young PC, Romanowicz R, *et al.* (2007) Uncertainty, sensitivity analysis and the role of data based mechanistic modelling in hydrology. *Hydrology and Earth System Sciences* **11(4)**: 1249–1266.

Refsgaard JC (1997) Validation and intercomparison of different updating procedures for real-time forecasting. *Nordic Hydrology* **28(2)**: 65–84.

Romanowicz RJ, Young PC and Beven KJ (2006) Data assimilation and adaptive forecasting of water levels in the River Severn catchment, United Kingdom. *Water Resources Research* **42(6)** W06407 **doi**:10.1029/2005WR004373.

Seibert J (2003) Reliability of model predictions outside calibration conditions. *Nordic Hydrology* **34(5)**: 477–492.

Smith MB, Laurine DP, Koren VI, Reed SM and Zhang Z (2003) Hydrologic model calibration in the National Weather Service. In *Water Science and Application 6: Calibration of Watershed Models* (Duan Q, *et al.* (eds)). American Geophysical Union, Washington, DC, pp. 133–152.

Taylor CJ, Pedregal DJ, Young PC and Tych W (2007) Environmental time series analysis and forecasting with the Captain toolbox. *Environmental Modelling & Software* **22(6)**: 797–814.

Vehviläinen B, Huttunen M and Huttunen I (2005) Hydrological forecasting and real time monitoring in Finland: The watershed simulation and forecasting system (WSFS). *Proceedings of International Conference on Innovation Advances and Implementation of Flood Forecasting Technology, Tromsø*. See www.actif-ec.net/conference2005/proceedings/index.html for further details (accessed 04/06/2010).

Wagener T, Lees MJ and Wheater HS (2002) A toolkit for the development and application of parsimonious hydrological models. In *Mathematical Models of Large Watershed*

Hydrology (Singh VP and Frevert DK (eds)). Water Resources Publications, Littleton, CO, pp. 91–132.

Weerts AH and El Serafy GYH (2006) Particle filtering and ensemble Kalman filtering for state updating with hydrological conceptual rainfall–runoff models. *Water Resources Research* **42(9)**: W09403.

Werner M and van Dijk M (2005) Developing flood forecasting systems: examples from the UK, Europe and Pakistan. *Proceedings of International Conference on Innovation Advances and Implementation of Flood Forecasting Technology, Tromsø*. See http://www.actif-ec.net/conference2005/proceedings/index.html for further details (accessed 04/06/2010).

Wheater HS and Peach D (2004) Developing interdisciplinary science for integrated catchment management: the UK LOwland CAtchment Research (LOCAR) programme. *Water Resources Development* **20(3)**: 369–385.

Wheater HS, Jakeman AJ and Beven KJ (1993) Progress and directions in rainfall–runoff modelling. In *Modelling Change in Environmental Systems* (Jakeman AJ, Beck MB and McAleer MJ (eds)). Wiley, Chichester, pp. 101–132.

Whitfield D (2005) The National Flood Forecasting System (NFFS) of the UK Environment Agency. *Proceedings of International Conference on Innovation Advances and Implementation of Flood Forecasting Technology, Tromsø*. See http://www.actif-ec.net/conference2005/proceedings/index.html for further details (accessed 05/03/2009).

Young PC (1984) *Recursive Estimation and Time-series Analysis: An Introduction*. Springer, Berlin.

Young P (1998) Data-based mechanistic modelling of environmental, ecological, economic and engineering systems. *Environmental Modelling & Software* **13(2)**: 105–122.

Young PC (2002) Advances in real-time flood forecasting. *Philosophical Transactions of the Royal Society Series A* **360(1796)**: 1433–1450.

Young PC (2003) Top-down and data-based mechanistic modelling of rainfall-flow dynamics at the catchment scale. *Hydrological Processes* **17(11)**: 2195–2217.

Young PC (2004) Identification and estimation of continuous-time hydrological models from discrete-time data. In *Hydrology: Science and Practice for the 21st Century, Volume 1* (Webb B, *et al.* (eds)). British Hydrological Society, London, UK, pp. 406–413.

Young PC (2006a) Data-based mechanistic modelling and river flow forecasting. *Proceedings of 14th IFAC Symposium on System Identification, Newcastle, Australia*, pp. 756–761. See www.ifac-papersonline.net/detailed/25481.html (accessed 01/12/2011).

Young PC (2006b) The data-based mechanistic approach to the modelling, forecasting and control of environmental systems. *Annual Reviews in Control* **30(2)**: 169–182.

Young PC (2007) Real-time flow forecasting. In *Hydrological Modelling in Arid and Semi-arid Areas* (Wheater HS, Sorooshian S and Sharma KD (eds)). Cambridge University Press, Cambridge, pp. 113–137.

Young PC and Beven KJ (1994) Data-based mechanistic modelling and the rainfall-flow non-linearity. *Envirometrics* **5(3)**: 335–363.

Young PC and Garnier H (2006) Identification and estimation of continuous-time, data-based mechanistic (DBM) models for environmental systems. *Environmental Modelling & Software* **21(8)**: 1055–1072.

Young PC and Tomlin CM (2000) Data-based mechanistic modelling and adaptive flow forecasting. In *Flood Forecasting: What does Current Research offer the Practitioner? BHS National Meeting, University of Bristol*. (Lees M and Walsh P (eds)). British Hydrological Society, London, Occasional paper 12, pp. 25–39. See www.hydrology.org.uk/publications/bhs_op121.pdf (accessed 01/12/2011).

Young PC, McKenna P and Bruun J (2001) Identification of non-linear stochastic systems by state dependent parameter estimation. *International Journal of Control* **74(18)**: 1837–1857.

Young PC, Romanowicz R and Beven K (2006) *Updating Algorithms in Flood Forecasting*. Flood Risk Management Research Consortium, Research report UR5. See www.floodrisk.org.uk/images/stories/phase1/UR5%20signed%20off.pdf (accessed 01/12/2011).